NANO LETTERS

2007
Vol. 7, No. 1
155−160

Effects of Mechanical Flexion on the Penetration of Fullerene Amino Acid-Derivatized Peptide Nanoparticles through Skin

Jillian G. Rouse,[†,‡] Jianzhong Yang,[§] Jessica P. Ryman-Rasmussen,[†] Andrew R. Barron,[§] and Nancy A. Monteiro-Riviere*[,†,‡]

Center for Chemical Toxicology Research and Pharmacokinetics, Department of Clinical Sciences, and Department of Biomedical Engineering, North Carolina State University, 4700 Hillsborough Street, Raleigh, North Carolina 27606, and Department of Chemistry and the Richard E. Smalley Institute for Nanoscale Science and Technology, Rice University, Houston, Texas 77005

Received October 19, 2006; Revised Manuscript Received November 22, 2006

ABSTRACT

Dermatomed porcine skin was fixed to a flexing device and topically dosed with 33.5 mg·mL^{-1} of an aqueous solution of a fullerene-substituted phenylalanine (Baa) derivative of a nuclear localization peptide sequence (Baa-Lys(FITC)-NLS). Skin was flexed for 60 or 90 min or left unflexed (control). Confocal microscopy depicted dermal penetration of the nanoparticles at 8 h in skin flexed for 60 and 90 min, whereas Baa-Lys-(FITC)-NLS did not penetrate into the dermis of unflexed skin until 24 h. TEM analysis revealed fullerene-peptide localization within the intercellular spaces of the stratum granulosum.

The ability of quantum dots and fullerenes to penetrate intact skin[1,2] provides potential benefits for the development of nanomaterial applications involving drug delivery. For these developments to occur, it is important to fully understand the mechanisms through which nanoparticles traverse skin and to determine external factors that contribute to increased penetration. Many processes in the occupational environment, for example, involve repetitive motions that accentuate naturally occurring biomechanical forces and alter the body's ability to perform certain physiological functions.[3] Mechanical stimulation that occurs during these repetitive motions may alter the structural organization of skin and lead to increased penetration of nanoparticles by compromising the permeability barrier of the epidermis.

The high prevalence of podoconiosis in the African rift valleys due to exposure of unprotected feet to soils with high concentrations of zirconium and beryllium[4,5] led Tinkle et al. to investigate the relationship between particle penetration and mechanical stressors.[6] These results showed a direct correlation between particle penetration and a flexing movement used to simulate pressure applied by walking barefoot[6] and suggest that forces applied to skin during standard physiological processes, such as walking, can influence dermal exposure and lead to increased penetration. To investigate the relationship between nanoparticle penetration and biomechanical loading, a fullerene-substituted peptide, Baa-Lys(FITC)-NLS was synthesized, and its penetration through flexed and unflexed skin was observed.

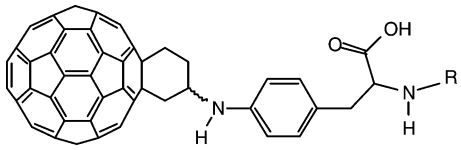

R = H (Baa, **1a**); C(O)O^{t}Bu (N-Boc-Baa, **1b**)

Figure 1.

We have previously reported the synthesis of the phenylalanine-based fullerene amino acid, Bucky amino acid[7] (Baa, Figure 1a), and the uptake and interaction of Baa with human epidermal keratinocytes (HEK).[8] The presence of the fullerene substituent has a significant effect on the intracellular transport of peptides containing Baa. The addition of a fullerene-derived amino acid to a cationic peptide results in

* To whom correspondence should be addressed. E-mail address: Nancy_Monteiro@ncsu.edu. Telephone: 919-513-6426. Fax: 919-513-6358.

† Center for Chemical Toxicology Research and Pharmacokinetics, Department of Clinical Sciences, North Carolina State University.

‡ Department of Biomedical Engineering, North Carolina State University.

§ Department of Chemistry and the Richard E. Smalley Institute for Nanoscale Science and Technology, Rice University.

10.1021/nl062464m CCC: $37.00 © 2007 American Chemical Society
Published on Web 12/06/2006

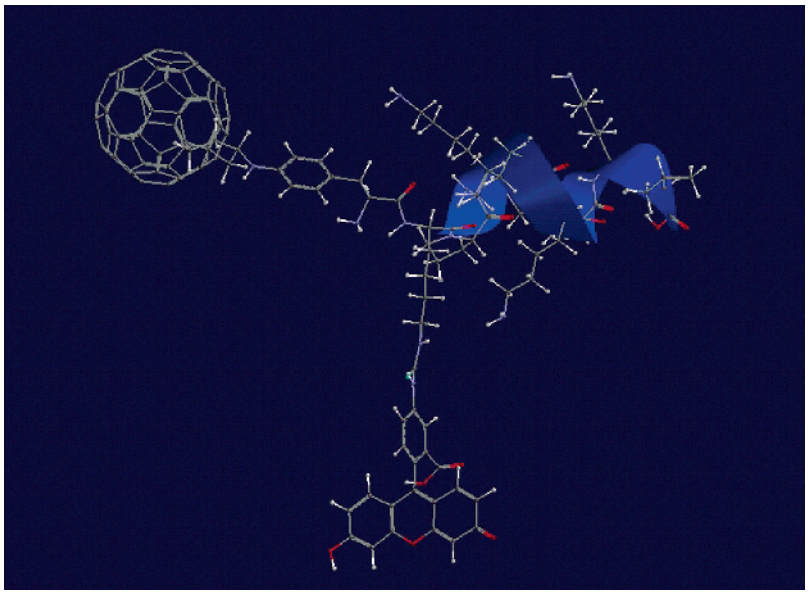

Figure 2. Calculated structure of Baa-Lys(FITC)-NLS showing the special relationship between the C_{60} and FITC residues.

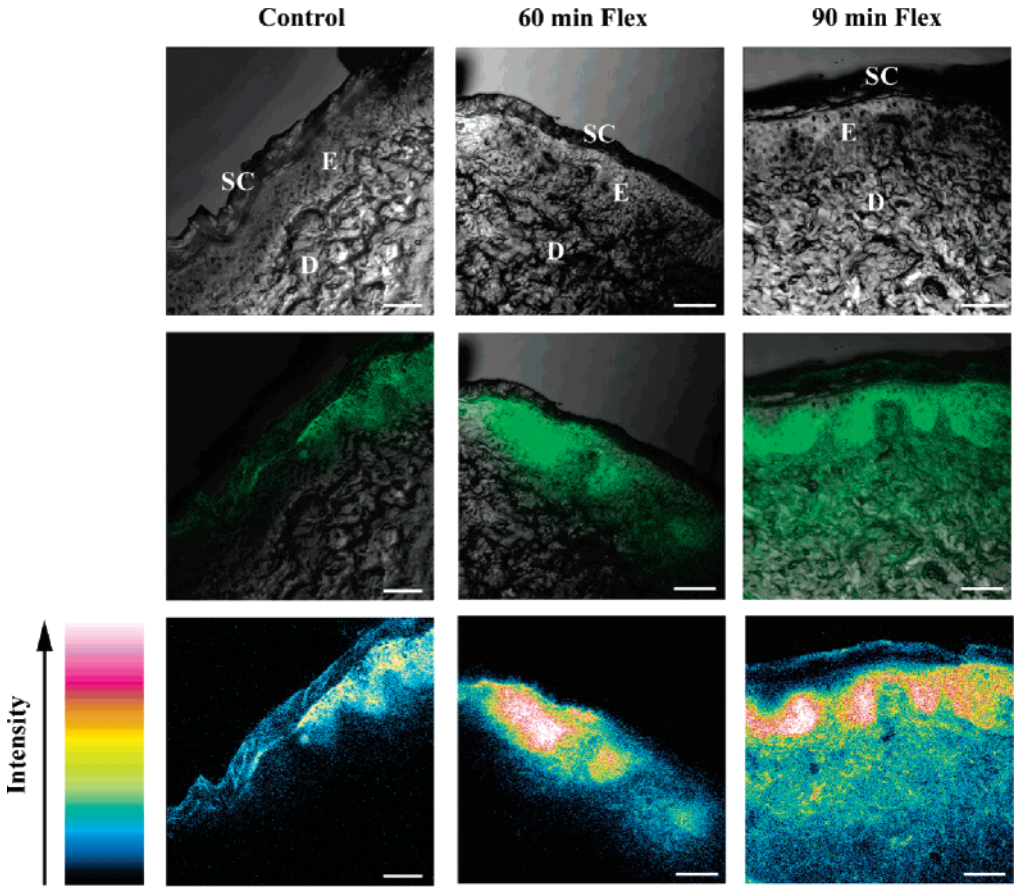

Figure 3. Confocal scanning microscopy images of intact skin dosed with Baa-Lys(FITC)-NLS for 8 h. Top row: confocal-DIC channel image shows an intact stratum corneum (SC) and underlying epidermal (E) and dermal layers (D). Middle row: Baa-Lys(FITC)-NLS fluorescence channel (green) and confocal-DIC channel show fullerene penetration through the epidermal and dermal layers of skin. Bottom row: fluorescence intensity scan showing Baa-Lys(FITC)-NLS penetration. All scale bars represent 50 μm.

the peptide showing cellular uptake, whereas the same peptide sequence in the absence of Baa shows no transport across the cell membrane.[9] One peptide sequence that shows particular facile intracellular transport is based on the nuclear localization sequence (NLS, primary sequence H-Pro-Lys−Lys-Lys-Arg-Lys-Val-OH). The stability of the fullerene linkage and the ability to prepare peptides with a fluorescent tag allows for investigation of the transport of a bio−nano conjugate through skin.

The couplings of normal amino acid sequence without Baa was carried out on an automated peptide synthesizer using preloaded Fmoc-Val-Wang resin as the solid phase.[10] After

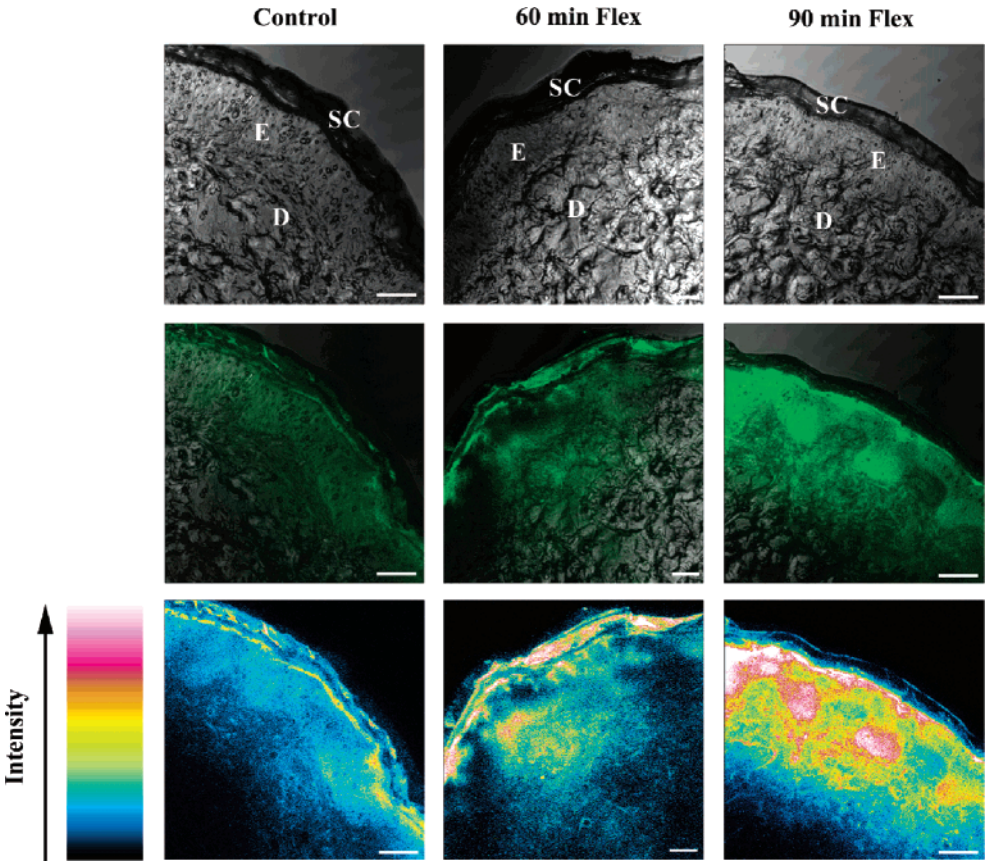

Figure 4. Confocal scanning microscopy images of skin dosed with Baa-Lys(FITC)-NLS for 24 h. Top row: confocal-DIC channel image shows an intact stratum corneum (SC) and underlying epidermal (E) and dermal layers (D). Middle row: Baa-Lys(FITC)-NLS fluorescence channel (green) and confocal-DIC channel show fullerene penetration through the skin. Bottom row: fluorescence intensity scan of Baa-Lys(FITC)-NLS. All scale bars represent 50 μm.

the NLS sequence (Pro-Lys−Lys-Lys-Arg-Lys-Val) was completed, a Lys(Mtt) residue was coupled to the end to allow attachment of the fluorescein isothiocyanate (FITC) fluorescent marker. The coupling with N-Boc-Baa (Figure 1b)[11] was performed manually.[10] Cleavage from the resin followed by RP-HPLC purification yielded the fullerene substituted peptide, Baa-Lys(FITC)-NLS (Figure 2).[12] Before functionalization, the individual fullerenes were, on average, 0.7 nm in size. Individual Baa-Lys(FITC)-NLS particles are *ca.* 3.5 nm.

Because of its physiological and structural similarities to human skin,[13−16] porcine skin was used a model for human skin in this study. The care and experimental use of all pigs were in accordance with the North Carolina State University Institutional Animal Care and Use Committee (IACUC). Pigs were sacrificed by intravenous injection of 100 mg/kg Euthasol (Delmarva Laboratories, Inc., Midlothian, VA), and the skin was dermatomed at a thickness of 400 μm. The dermatomed skin was fixed to a flexing apparatus designed to flex skin at $\pm$ 45° and at a frequency of 20 flexes·min^{-1} (a detailed description of the flexing device can be found in Supporting Information).

To determine the effects of flexing on skin penetration, the dermatomed skin was dosed with 20 μL of Baa-Lys-(FITC)-NLS in 1% PBS (33.5 mg·mL^{-1}), and the dosed areas were subsequently flexed for 60 or 90 min or left unflexed (control). In pilot studies, skin flexed for either 15 or 30 min and dosed with radiolabeled methyl parathion showed no evidence of increased penetration in comparison to unflexed samples. Therefore, flex of times of 60 and 90 min were chosen to investigate nanoparticle penetration. After the allotted flexing time, percutaneous absorption was assessed using a flow-through diffusion cell system.[17,18] Temperature and pH of the perfusate (1.2 mM KH_2PO_4, 32.7 mM $NaHCO_3$, 2.5 mM $CaCl_2$, 4.8 mM KCl, 1.2 mM $MgSO_4$·$7H_2O$, 118 mM NaCl, 1200 mg.L^{-1} D-glucose, 4.5% BSA, 5 U/mL heparin, 30 μg·mL^{-1} amikacin, and 12.5 U·mL^{-1} penicillin G) were monitored and kept constant at 37 °C and pH 7.4. The diffusion cells were run at 1.75 mL·min^{-1} for either 8 h or 24 h. Immediately after each time point, the samples were bisected along the flex line and either frozen at −80 °C for later sectioning or placed in Trump's fixative at 4 °C for transmission electron microscopy (TEM). Confocal microscopy and TEM were used to visualize Baa-Lys(FITC)-NLS penetration (see Supporting Information). At least three diffusion cells were run for each flex time and exposure time.

For each experimental treatment, Baa-Lys(FITC)-NLS had penetrated the skin by 8 h (Figure 3). The fullerenes were localized primarily in the epidermal layers of non-flexed

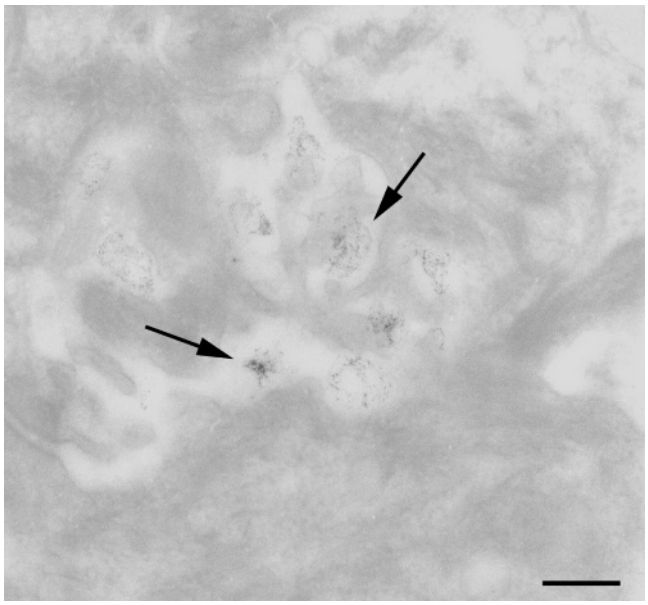

Figure 5. Unstained transmission electron microscopy image of Baa-Lys(FITC)-NLS (arrows) localization at 24 h in skin flexed for 90 min. The fullerenes are present within the intercellular space of the stratum granulosum cell layer (shown by the arrows). The scale bar represents 300 nm.

(control) skin, whereas the 60 and 90 min flexed samples showed evidence of greater epidermal (60 min) and dermal (90 min) penetration (Figure 3, middle row). Skin flexed for 90 min had a substantially greater amount of Baa-Lys(FITC)-NLS dermal penetration than non-flexed skin (control) and 60 min flexed skin. The DIC images (Figure 3, top row) depict an intact stratum corneum, which provides evidence that nanoparticle penetration did not occur as a result of skin abrasion. The fluorescence of Baa-Lys(FITC)-NL as it moves through the skin can be seen in Figure 3, middle row. The fluorescence intensity maps (Figure 3, bottom row) reveal a concentration gradient of the Baa-Lys(FITC)-NLS, ranging from a high concentration of particles in the epidermis (white) to a low concentration in the dermal layers (blue). Images are representative of two separate experiments performed in triplicate.

After 24 h of Baa-Lys(FITC)-NLS treatment, skin penetration was greater in all experimental groups (Figure 4). Again, the DIC images reveal a thick, intact stratum corneum and the intensity maps show the highest concentration of particles in the upper epidermal layers and a lower concentration as the fullerenes penetrate into the dermis. Skin flexed for 90 min showed the greatest amount of dermal penetration, evident by the higher fluorescence intensity of the nanoparticles in this group (Figure 4, bottom row). It is important to note that for all treatments nanoparticle penetration was non-homogeneous probably due to a nonuniform distribution of the dose over the dose region and/or differences in the thickness of the epidermis. The images presented are representative of the trends seen for each set of treatments.

TEM further verifies that Baa-Lys(FITC)-NLS is capable of penetrating intact skin and localizing between keratinocytes. Figure 5 is a representative image of skin flexed for 90 min that depicts localization of the fullerene within the intercellular space of the stratum granulosum cell layer at 24 h.

This study investigated the effects of mechanical flexion on the penetration of fullerenes through intact skin. In developing new applications involving nanomaterials and nanoparticles, it is important to adequately assess all factors that can lead to increased nanoparticle exposure. Previous research has already demonstrated that nanoparticles can penetrate skin cells[8,19] and intact skin;[1,2] the aim of this study is to identify factors that can lead to increased penetration and/or rate of penetration. Evaluation of these factors is of interest for the development of nanodrug delivery applications and in identifying occupational hazards that arise during manufacturing processes and repeated exposure to nanoparticles. Since recent research has identified the potential toxicity of some nanoparticles,[8,19−23] these results could have profound implications for researchers, manufacturers and medical personnel alike.

The mechanical loading regimes used in this study attempt to mimic physiological forces that can occur during nanoparticle manufacturing processes or conditions involved in consumer use. The external forces applied to the skin while flexing proves to have a significant effect on both the rate and extent of fullerene penetration. Skin flexed for 90 min shows evidence of dermal penetration after 8 h of nanoparticle exposure, whereas control specimens show evidence of fullerenes primarily localized in the epidermis and only a slight amount in the dermis after the 24 h treatment. These results suggest that the action of a flexing procedure increases the rate at which fullerenes can penetrate through the skin. Furthermore, flexing increased the amount of fullerenes that were capable of penetrating into the dermal layers of skin, indicated by the higher fluorescence intensity of fullerenes for both 60 and 90 min flexed skin.

The route of nanoparticle penetration through the skin is of great interest, especially in the nanomedicine field. In this study, TEM depicted derivatized fullerenes localized within intercellular spaces of the epidermis, suggesting that migration through the skin occurs intercellularly as opposed to movement through cells. Additionally, the concentration gradients of fullerenes between the epidermis and dermis shown in the fluorescence intensity maps of Figures 3 and 4 indicate that fullerene penetration occurs via a mechanism of passive diffusion. Therefore, movement of the derivatized nanoparticles through the skin is dependent on the hydrophobic lipid entities that are present between the epidermal cells. These intercellular lipids are arranged into lamellar sheets and, typically, responsible for the permeability barrier of the skin.[24] The ability of the nanoparticles to traverse through these lipid lamellae and to enter into the dermis of skin indicates that nanomaterials could get absorbed by the capillaries of the papillary layer with the potential to localize elsewhere in the body.[21] For drug-delivery applications, the ability of nanoparticles to have access to systemic circulation has important implications. However, because some nanoparticles have been shown to initiate adverse biological responses,[8,19−23] there are potential risks for systemic toxicity

to occur and, therefore, the need arises for risk assessment and the establishment of safety regulations.

At present, the mechanisms through which flexing increases nanoparticle penetration are unknown. Dynamic light scattering and cryo-TEM analyses were conducted in order to determine the particle size in solution and to determine its relationship to transport through skin (refer to Supporting Information for procedure details). On the basis of these techniques, it was found that in solution Baa-Lys(FITC)-NLS forms spherical and ellipsoidal clusters with average aggregate sizes of approximately 40−250 nm. On the basis of previous knowledge that the vertical and lateral gaps between corneocytes present in the stratum corneum are about 19 nm,[26] it seems likely that the larger Baa-Lys(FITC)-NLS aggregates based on conformational shape would have limited capabilities of diffusing through the epidermal layers via intercellular spaces. It is evident from the results of this study, however, that the fullerene-based peptides do penetrate through the epidermal layers via passive diffusion and that flexing increases this penetration. Since external mechanical stimuli are transmitted to individual cells,[27,28] it is possible to speculate that the forces applied to the skin during flexing cause changes in the morphology and architectural lipid organization of the upper epidermal layers. A transient increase in the size of the intercellular spaces during mechanical stimulation could be responsible for the increase in penetration seen in skin samples flexed for 60 and 90 min.

This study confirms that fullerene-based peptides can penetrate intact skin and that mechanical stressors, such as those associated with a repetitive flexing motion, increase the rate at which these particles traverse into the dermis. These results are important for identifying external factors that increase the risks associated with nanoparticle exposure during manufacturing or consumer processes. Future assessments of nanoparticle safety should recognize and take into account the effect that repetitive motion and mechanical stressors have on nanoparticle interactions with the biological environment. Additionally, these results could have profound implications for the development of nanoparticle use in drug-delivery, specifically in understanding mechanisms by which nanoparticles penetrate intact skin.

Acknowledgment. Supported by the US EPA-STAR Program #RD-83171501-0 (N.A.M.-R.), the National Academies Keck Futures Initiative (N.A.M.-R. and A.R.B.), and the Robert A. Welch Foundation (A.R.B.). The authors thank Alfred Inman and all of the staff of the Center for Chemical Toxicology Research and Pharmacokinetics at North Carolina State University for their technical assistance.

Supporting Information Available: Text giving a description of the flexing apparatus, confocal microscopy, dynamic light scattering, and cryo-TEM techniques and figures showing a plot of the fraction of aggregates for Baa-Lys(FITC)-NLS as a function of solution concentration and vitreous ice cryo-TEM micrographs of the large and small aggregates formed. This material is available free of charge via the Internet at http://pubs.acs.org.

References

(1) Ryman-Rasmussen, J. P.; Riviere, J. E.; Monteiro-Riviere, N. A. *Toxicol. Sci.* **2006**, *91*, 159−165.
(2) Monteiro-Riviere, N. A.; Yang, J.; Inman, A. O.; Ryman-Rasmussen, J. P.; Barron, A. R.; Riviere, J. E. *Toxicol. Sci.* **2006**, *90*, 168.
(3) Barr, A. E. *Man. Therapy* **2006**, *11*, 173−174.
(4) Blundell, G.; Henderson, W. J.; Price, E. W. *Ann. Trop. Med. Parasitol.* **1989**, *83*, 381−385.
(5) Corachan, M.; Tura, J. M.; Campo, E.; Soley, M.; Traveria, A. *Trop. Geogr. Med.* **1988**, *40*, 359−364.
(6) Tinkle, S. S.; Antonini, J. M.; Rich, B. A.; Roberts, J. R.; Salmen, R.; DePree, K.; Adkins, E. J. *Environ. Health Perspect.* **2003**, *111*, 1202−1208.
(7) Yang, J.; Barron, A. R. *Chem. Commun.* **2004**, 2884−2885.
(8) Rouse, J. G.; Yang, J.; Barron, A. R.; Monteiro-Riviere, N. A. *Toxicol. In Vitro* **2006**, *20*, 1313−1320.
(9) Yang, J.; Wang, K.; Driver, J.; Yang, J.; Barron, A. R. *Org. Biomol. Chem.* **2007**, in press.
(10) Using preloaded Fmoc-Val-Wang resin (491 mg, 0.30 mmol) as solid phase, each coupling used 4 fold amino acid excess, and HBTU, HOBT as activators and DIEA as base in a 1:1:1:3 ratio. Fmoc deprotection was performed using 25% perperidine in DMF solution. After the NLS sequence (Pro-Lys-Lys-Lys-Arg-Lys-Val) was completed, a Lys(Mtt) residue was coupled to the end. One sixth of the resin was placed in a 25 mL fritted glass tube, swollen with DMF. A 3-fold excess of N-Boc-Baa (157 mg, 0.15 mM) dissolved in DMF/DCM (9 mL, 2:1) was activated with PyBOP/HOBt/DIEA (1:1:1:3) for 2 minutes, then mixed with the resin in the fritted glass tube, and shaken on an automated shaker for 1 day at room temperature. The resin was washed thoroughly with DMF and DCM to remove any unreacted N-Boc-Baa. The resin was washed with DCM for complete removal of DMF. To achieve the maximum cleavage of Mtt protecting group, the resin was shrunk with MeOH twice. When the resin was treated with 1% TFA and 5% TIPS in DCM 2 minutes for three times. The resin was washed again with DCM thoroughly, and swelled in DMF for 1 hour. Afterward the resin was shaken with a solution of FITC (65 mg) in DMF (8 mL) and DIEA (130 mL) overnight. At the end of the synthesis, the FITC labeled fullerene peptides was washed repeatedly with DMF, DCM and shrunk with MeOH. The resin was thoroughly dried over Dryrite in a vacuum oven overnight. The cleavage of the peptide was achieved with TFA/TIPS/H_2O (95:2.5:2.5) cocktail for 4 hr. After filtration, the peptide solution was concentrated by Rotavap at room temperature and precipitated with cold Et_2O. The crude was washed with diethyl ether two more times and, after centrifugation of the final wash, it was frozen and lyophilized. RP-HPLC purification was carried out on a Phenomenex Luna C5 column using an isocratic gradient of (A) 0.1% TFA in water and (B) 0.1% TFA in 2-propanol, 70% B, at 5.0 $mL \cdot min^{-1}$ flow rate. The elution time was 37 min. After purification 59.1 mg (50.6%) was recovered.
(11) Yang, J.; Alemany, L. B.; Driver, J.; Hartgerink, J. D.; Barron, A. R. *Chem.−Eur. J.* 2006, in press.
(12) MALDI-MS: *m/z* calculated 2337 [$M^+ + H$], 1948 [$M^+ + H-FITC$]; found 2337, 1948.
(13) Chilcot, R. P.; Dalton, C. H.; Hill, I.; Davison, C. M.; Blohm, K. L.; Clarkson, E. D.; Hamilton, M. G. *Hum. Exp. Toxicol.* **2005**, *24*, 347−352.
(14) Monteiro-Riviere, N. A. In *The Biology of the Domestic Pig*; Pond, W. G., Mersmann, H. G., Eds.; Cornell University Press: Ithaca, NY, 2001; pp 585−624.
(15) Schmook, F. P.; Meingassner, J. G.; Billich, A. *Int. J. Pharm.* **2001**, *215*, 51−56.
(16) Singh, S.; Zhao, K.; Singh, J. *Drug Chem. Toxicol.* **2002**, *25*, 83−92.
(17) Chang, S. K.; Riviere, J. E. *Fundam. Appl. Toxicol.* **1991**, *17*, 494−504.
(18) Bronaugh, R. L.; Stewart, R. F. *J. Pharm. Sci.* **1985**, *74*, 64−67.
(19) Monteiro-Riviere, N. A.; Nemanich, R.; Inman, A. O.; Wang, Y.; Riviere, J. E. *Toxicol. Lett.* **2005**, *155*, 377−384.
(20) Magrez, A.; Kasas, S.; Salicio, V.; Pasquier, N.; Seo, J. W.; Celio, M.; Catsicas, S.; Schwaller, B.; Forro, L. *Nano Lett.* **2006**, *6*, 1121−1125.
(21) Shvedova, A.; Castranova, V.; Kisin, E.; Schwegler-Berry, D.; Murray, A.; Gandlelsman, V.; Maynard, A.; Baron, P. *J. Toxicol. Environ. Health* **2003**, *66*, 1909−1926.
(22) Oberdorseter, E. *Enivron. Health Perspect.* **2004**, *112*, 1058−1062.

(23) Sayes, C. M.; Fortner, J. D.; Guo, W.; Lyon, D.; Boyd, A. M.; Ausman, K. D.; Tao, Y. J.; Sitharaman, B.; Wilson, L. J.; Hughes, J. B.; West, J. L.; Colvin V. L. *Nano Lett.* **2004**, *4*, 1881−1887.
(24) Monteiro-Riviere, N. A.; Riviere, J. E. In *Dermal Absorption Models in Toxicology and Pharmacology*; Riviere, J. E., Ed.; Taylor & Francis: New York, 2006; pp 1−8.
(25) Monteiro-Riviere, N. A.; Inman, A. O.; Riviere, J. E.; McNeill, S. C.; Francoeur, M. L. *Pharm. Res.* **1993**, *10*, 1326−1331.
(26) van der Merwe, D.; Brooks, J. D.; Gehring, R.; Baynes, R. E.; Monteiro-Riviere, N. A.; Riviere, J. E. *Toxicol. Sci.* **2006**, *89*, 188−204.
(27) Zahalak, G. I.; Wagenseil, J. E.; Wakatsuki, T.; Elson, E. L. *Biophys. J.* **2000**, *79*, 2369−2381.
(28) Guilak, F.; Mow, V. C. *J. Biomech.* **2000**, *33*, 1663−1673.

NL062464M